Research Article | Vol. 29, No. 10 / 10 May 2021 / Optics Express 15699
Optics EXPRESS

Design guidelines for ultrashort pulse generation by a Mamyshev regenerator

MIKKO NÄRHI,[1,*] ANDREI FEDOTOV,[1] KSENIIA AKSENOVA,[1,2] JULIA FIEBRANDT,[3] THOMAS SCHÖNAU,[3] MARIO GERECKE,[3] AND REGINA GUMENYUK[1]

[1]*Laboratory of Photonics, Tampere University, Kalevantie 4, Tampere 33100, Finland*
[2]*Peter the Great St. Petersburg Polytechnical University, Polytechnicheskaya ul. 29, 195251 St. Petersburg, Russia*
[3]*PicoQuant GmbH, Rudower Chaussee 29, 12489 Berlin, Germany*
[*]*mikko.narhi@tuni.fi*

Abstract: We study numerically the possibility of using various gain-switched seed laser pulse parameters and fibers for a low-cost, all-fiber Mamyshev regenerator scheme. We find that for increasing pulse durations, sufficient spectral broadening will be difficult to achieve in practice and careful design of the system parameters is required for the regenerator to function. Furthermore, an optimal input peak power level can be defined for a given fiber and pulse duration that results from a balance of competing Kerr effect and stimulated Raman scattering. We also demonstrate experimental results of 3 ps pulse generation seeded by an 80 ps gain-switched diode. Our results pave the way for designing pulse-on-demand picosecond scale fiber sources for applications.

1. Introduction

Pulsed laser sources with picosecond and femtosecond durations have enabled numerous applications in applied sciences such as materials processing [1,2] and LIDAR measurements [3,4] as well as opened up new frontiers in fundamental science by allowing straightforward access in experiments in nonlinear dynamics [5,6] and dual-comb spectroscopy [7,8]. The plethora of applications drive ultrafast laser source development continuously with new targets set in sight for cost-effectiveness, low footprint and turn-key and robust use. Fiber lasers are particularly well suited for this task due to the compact nature of the sources with necessary industrial ruggedness when all-fiber polarization maintaining configurations are used.

Mode-locking remains as the de-facto standard for generating ultrafast pulses in fibers. Mode-locking is typically achieved with either a real saturable absorber (e.g. semiconductor, graphite or carbon nanotubes) or an artifical saturable absorber (e.g. nonlinear polarization rotation, nonlinear fiber loop mirrors). Pulses obtained from mode-locked sources offer excellent pulse contrast and signal-to-noise ratio. These mode-locking schemes have different traits in terms of stability and lifetime and a suitable one can often be chosen depending on the requirements of the application. One characteristic common to all of these designs is that the repetition rate of the laser is fixed to the fundamental repetition rate set by the cavity length typically ranging in the 10-100 MHz range. Some applications such as materials processing would, however, benefit from tunable pulse repetition rate or even pulse-on-demand operation. For mode-locked lasers, various mechanisms such as harmonic mode-locking, multiplexers or acousto-optic pulse picking can usually be employed to slightly vary the repetition rate of the source [9–13]. However, these techniques have their limitations in what can be achieved, and they often result in additional cost and complexity for the final system. Thus an electronically controllable, pulse-on-demand source could provide new aspects for applications.

Recently, a new path towards coherent ultrafast pulse generation in fibers was proposed utilizing a Mamyshev regenerator scheme [14,15]. In the scheme an electronically controllable

#422431 https://doi.org/10.1364/OE.422431
Journal © 2021 Received 10 Feb 2021; revised 20 Apr 2021; accepted 29 Apr 2021; published 7 May 2021

Optics EXPRESS

gain-switched pulsed diode laser was launched into a passive optical fiber, where self-phase modulation (SPM) broadens the spectrum, so that a coherent part of the spectrum can be filtered out resulting in a cleaner pulse shape suitable for further pulse shaping. This is illustrated in Fig. 1.

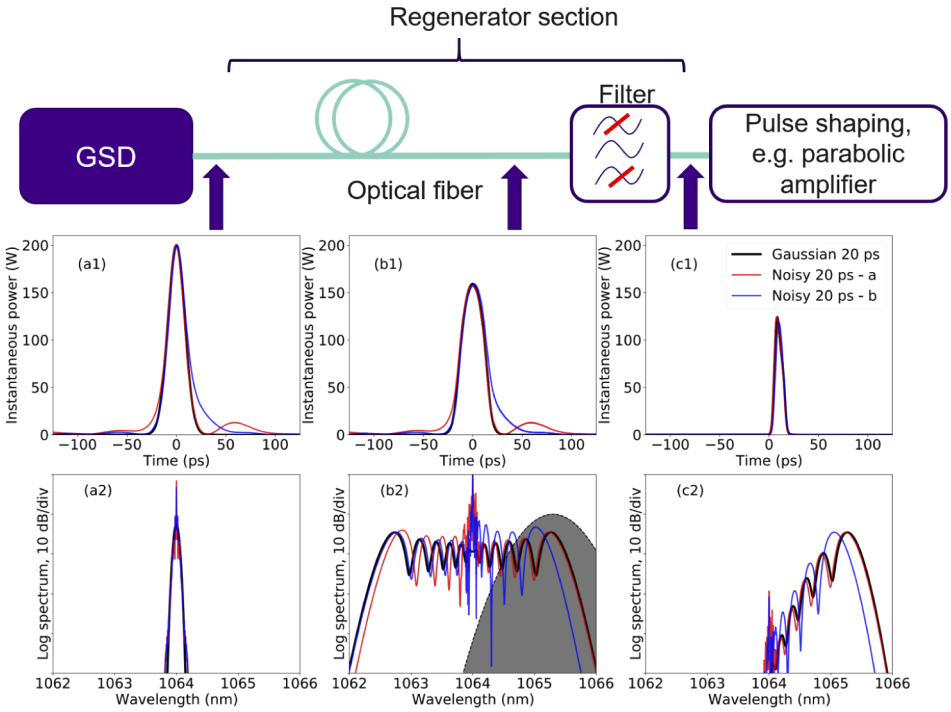

Fig. 1. High-level experimental schematic of a single Mamyshev Regenerator stage consisting of a noisy gain-switched diode laser, a long piece of passive fiber and a subsequent bandpass filter. Subfigures demonstrate pulse temporal and spectral evolution inside the regenerator starting at the GSD pulses (a), after propagation in fiber (b) and after filtering (c). We have compared a Gaussian pulse shape (black) to two noisy GSD pulse shapes (red and blue pulses with added random fluctuations) with the same peak power & duration. Filter is shown as the grayed area in (b2). Additional pulse shaping stages can be used after the regenerator scheme to achieve even shorter pulse durations than shown here.

The initially noisy pulses from the gain-switched laser diode (GSD) will broaden the spectrum sufficiently, so that when a part of the spectrum is filtered out, it will clean the pulse shape and increase coherence. However, for successful filtering that cleans the pulse, spectral broadening of several nanometers has to be achieved. In contrast to traditional mode-locked oscillators or recently presented femtosecond Mamyshev oscillators [16–19], the regenerator scheme requires no laser cavity to produce the pulses. Thus, such source could provide a simple, pulse-on-demand or tunable repetition rate operation with increased coherence, reduced pulse duration compared to conventional GSD solutions. The details of the scheme presented in Fig. 1 will be discussed later.

Initial demonstration of the scheme [14] used a gain-switched diode with 10 ps pulse duration, that could be compressed down to 135 fs after the regenerator and following pulse shaping stages. However, such pulse durations represent the state-of-the art GSD performance and cost-reduction in such cases becomes questionable. In this article we present experimental demonstration of pulse shortening to roughly 3 ps seeded by 80 ps GSD pulses and a thorough numerical study on

Optics EXPRESS

the practical limitations of GSD seeded Mamyshev regenerators. In particular we concentrate in the simulations on the launched pulse duration, peak power and fiber parameters. The results demonstrate the viability of the scheme even with moderate GSD pulse durations if care is taken with adjusting the input peak power.

2. Experimental results

To verify whether pulse shortening is achievable with noisy and relatively long seed pulse durations in a Mamyshev regenerator scheme and to justify some of the approximations made in our numerical model, we built an experimental setup as illustrated in Fig. 2.

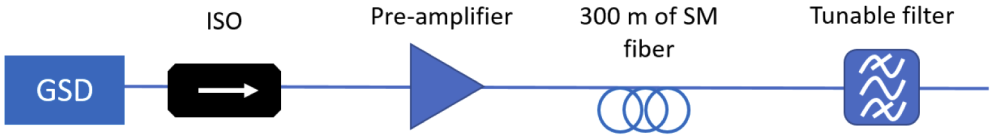

Fig. 2. Schematic of a GSD based Mamyshev Regenerator. The output of the GSD is amplified in a highly doped (absorption >85 dB/m @ 915 nm) pre-amplifier fiber pumped by a 976 nm diode. Non-PM fiber with 300 m length and MFD of 5.2 μm is spliced after the amplifier, which is followed by a tunable bandpass filter.

The seed laser was an 80 ps GSD from PicoQuant (CPDL-S-F-1064) that produced 23 μW at 1 MHz repetition rate with a center wavelength of 1063.2 nm. The output of the GSD was amplified in a short fiber pre-amplifier allowing us to scale the peak power of the pulses in experiments between 1 - 150 W. The seed and amplifier were PM-fiber based, but were coupled to a 300 m of non-PM fiber with a mode-field diameter of 5.2 μm for our tests. This non-PM fiber was chosen to reduce the Raman gain in the fiber due to polarization scrambling and because it was long enough to achieve sufficient spectral broadening for further filtering and compression. Furthermore, our simulations indicated this to be close to the optimum length with our pulse parameter range. The nonlinear effects and fiber length optimization will be discussed in more detail in the following sections.

The setup is fundamentally similar to the one presented by Fu *et al.* [14]. The major differences are the longer pulse duration of the diode (80 ps vs. 10 ps) as well as using longer and non-PM passive fiber segments for pulse broadening (300 m vs. 30 m). The achieved spectral broadening is smaller in our case due to the difference in pulse durations, being approximately 4 nm (vs. 7.5 nm). This limits our flexibility for tuning the filter as the incoherent central part of the spectrum has to be suppressed by the filter. Therefore, in contrast to Fu *et al.*, the filter in our case has to be placed near the edge of the spectrum where pulse fluctuations can be enhanced.

We start by demonstrating the behavior of the output spectrum of the GSD after propagating through the 300 m spool with increasing input peak power in Fig. 3. This corresponds to a typical experimental scenario, where the fiber length is fixed and the power can be adjusted by increasing the pre-amplifier pump current.

For low peak powers the system shows nearly no spectral broadening. Only after the peak power has increased above 40 W we start to see symmetrical broadening due to SPM. Increasing the power, the spectrum continues to broaden as nonlinear effects increase and we simultaneously see the stimulated Raman scattering (SRS) peak appear at around 1115 nm in Fig. 3(b). At the highest peak power of 148 W the SRS peak is already at −8 dB level relative to the spectral maximum, and it starts to affect the symmetry of the spectral broadening, with the long wavelengths suffering losses due to combined effects of depletion by SRS and cross-phase modulation [20]. We also note the increasing spectral contribution at 1030 nm, that is a typical characteristic of ASE increasing in a non-saturated ytterbium doped fiber amplifier.

Optics EXPRESS

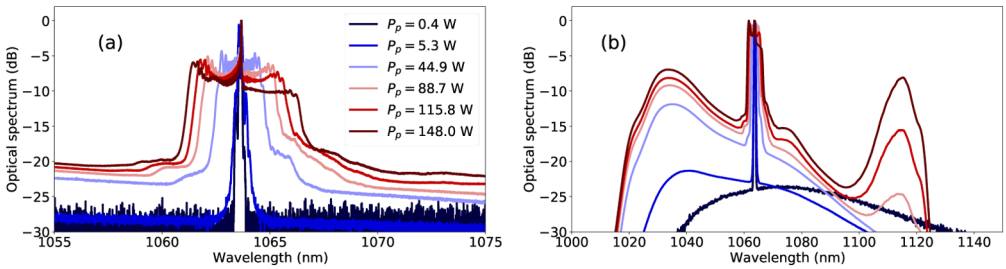

Fig. 3. Optical spectra recorded at the output of 300 m of non-PM fiber with increasing peak power: (a) High resolution spectra. The peak in the middle is caused by the incoherent fluctuations of the GSD laser. (b) Wide-bandwidth, low resolution spectra demonstrating the growth of the Raman sidebands (1110 nm) with increasing peak power. Peak at 1030 nm is ASE from the pre-amplifier.

In order to maintain the SRS levels moderate, we used approximately 110 W of peak power (10 mW of average power) after amplification at the input of the fiber spool. After the 300 m spool of fiber, a fiber coupled bandpass filter with approximately super-Gaussian filter shape and FWHM of 1.2 nm was used to carve out a part of the spectrum centered at 1065 nm. Average power dropped to 7 mW after the 300 m spool and consequently to 1 mW after the filter due to the filter intrinsic losses (3 dB) and a large part of the spectral power density being filtered out. A grating compressor in the Treacy configuration was used to verify compressibility of the pulses in conjunction with a scanning autocorrelator. Figure 4(c) and (d) demonstrate the filtered spectrum and autocorrelation data of the input GSD and after compression. We have chosen the peak power of 90 W to correspond to the case where Raman is still not affecting the pulse dynamics significantly.

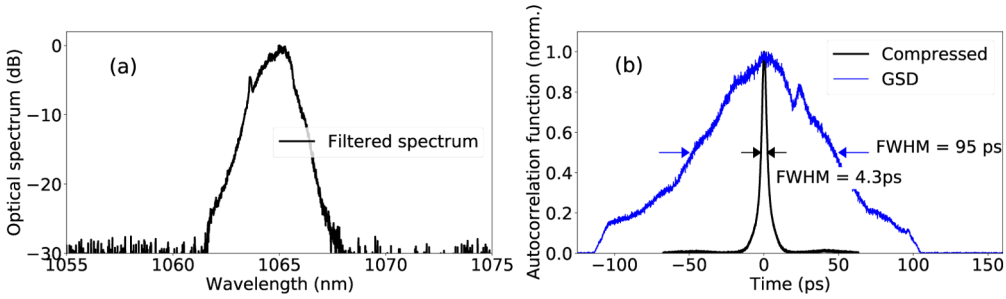

Fig. 4. (a) Filtered spectrum after by 1.2 nm bandpass filter. The peak on the left edge of the spectrum is the residual noise of the GSD. (b) autocorrelation of original GSD pulse (blue) and the compressed pulse after filtering (black).

The input autocorrelation is very noisy and asymmetric (which points to fluctuations or measurement error in the autocorrelation measurement) and has a FWHM duration 95 ps. After broadening in the fiber, the pulse achieves a spectral width of approximately 4.2 nm, which after filtering to 1.2 nm can be compressed down to 4.3 ps (autocorrelation FWHM), which assuming a Gaussian deconvolution factor of 1.414 corresponds to roughly to 3 ps of average pulse duration. This demonstrates the potential of the Mamyshev regenerator scheme even with longer pulses.

We point out that all of these measurements are *averaged*. In practice the pulse-to-pulse spectral widths will vary, and consequently the filtered pulse energies and durations will also fluctuate. Filtering at the edge of the spectrum is the most prone to these variations and performance of

Optics EXPRESS

the system will depend largely on the GSD fluctuations. Due to practical limitations we had to choose filtering near the edge in our experiments. In particular, we could not use smaller filter bandwidths in experiments that would allow us to filter more carefully between the noisy center peak of the GSD and the edge of the spectrum. As the spectral broadening was also limited with our GSD pulses, we had to resort to filtering nearly half of the broadened spectrum. We note that this increased the pulse amplitude fluctuations, but this was not quantified in more detail. Indeed, careful engineering of the system parameters: pulse duration, peak power, fiber length, fluctuations, filter position & bandwidth are required for the reliable operation of regenerator system. In the following sections we concentrate on optimizing the pulse parameters and fiber length by numerical simulations.

3. Numerical model and pulse dynamics

For the Mamyshev regenerator scheme to function, the spectral broadening of the GSD pulse has to be sufficient so that a coherent part of the spectrum can be carved out by the spectral filter. Thus a natural metric for the suitability of a scheme for practical purposes is the obtained spectral bandwidth at the output of the regenerator. Intuitively, one would just assume higher pulse powers to result in larger SPM induced spectral broadening and therefore better performance. However, increased peak power also changes the growth rate of detrimental stimulated Raman scattering (SRS) arising from noise that will eventually destroy the pulse temporal shape and affect spectral broadening, and thus preventing any subsequent filtering efforts in the regenerator scheme. Thus careful selection of pulse and fiber parameters is essential.

While analytical formulas can be given for SPM spectral broadening and Raman growth rate, these formulas are usually only valid in special cases where dispersive or nonlinear effects dominate [20]. In order to evaluate the simultaneous impact of the various nonlinear effects and dispersion on the pulse propagation we use numerical simulations based on solving the generalized nonlinear Schrödinger equation (GNLSE) by the split-step Fourier method [20,21]

$$\frac{\partial E}{\partial z} - \sum_{k=2,3} i^{k+1} \frac{\beta_k}{k!} \frac{\partial^k E}{\partial T^k} = i\gamma \left(1 + i\tau_{\text{shock}} \frac{\partial}{\partial T}\right) \left(E \int_{-\infty}^{\infty} R(t') |E(z, T - t')|^2 dt'\right). \tag{1}$$

Here $E(z, T)$ is the complex electric field envelope propagating in the co-moving time-frame of the pulse, β_k are the dispersion values up to third order, γ is the nonlinear coefficient of the fiber, $R(t)$ is the experimentally measured Raman response function and τ_{shock} is the self-steepening effect [21,22].

Initially, we performed some simulations with noisy pulse trains (Gaussian pulse with added broadband noise, see Fig. 1 for illustration) and compared the spectral broadening to transform limited Gaussian pulses of the same duration. We discovered, that the average spectrum of the noisy pulses corresponds roughly to the spectral broadening of transform limited pulses. We also simulated the propagation of 80 ps Gaussian pulses in 300 m of non-PM fiber with 150 W of peak power, corresponding to the experimental data shown in Fig. 3. The output spectra of the simulation is compared to the experimental data in Fig. 5. To initiate SRS growth in simulations, 300 photons per simulation frequency bin with random phase are used to generate the noisy background. This value is based on achieving a reasonable agreement with Raman values observed in the lab with the 80 ps GSD pulses. The simulation grid consisted of 2^{16} points on a 1.2 ns time window.

Encouraged by the agreement of simulations with experiments, we decided to use only transform limited Gaussian pulses with varying durations as the input pulses in the simulations presented in the manuscript in order to reduce computation time and to make the analysis more straightforward.

Simulations were performed for four different pulse durations: 20 ps, 50 ps, 80 ps and 100 ps with peak powers ranging from 50 W to 800 W centered at 1064 nm. In addition to this we studied

Optics EXPRESS

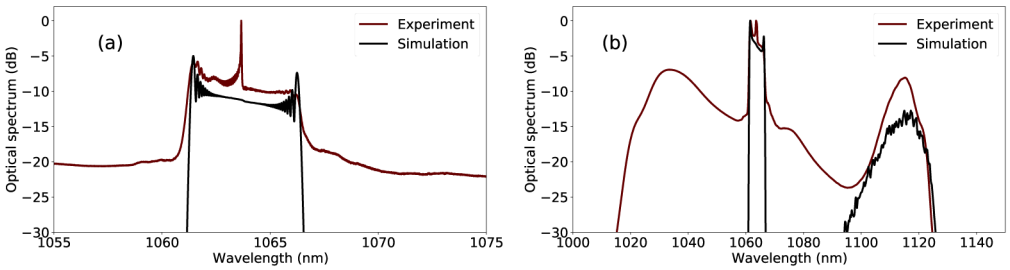

Fig. 5. Comparison of experimental (red) and simulated (black) results at the output of 300 m of non-PM fiber with 80 ps GSD pulses. (a) High resolution optical spectra. (b) Wide bandwidth, low resolution spectra demonstrating similar levels of SRS signal. Note that the Gaussian pulse simulations did not contain any ASE that affects the noise-floor in the spectral measurements.

the effect of choosing a different fiber type for obtaining optimal performance. The group velocity dispersion coefficient β_2 ranged from 0.018 ps^2 to 0.03 ps^2 in the normal dispersion regime and the effective area of the fiber ranged between 5-10 μm affecting the nonlinear coefficient according to $\gamma = n_2\omega_0/(cA_{\text{eff}})$ [20]. We have also simulated polarization-maintaining (PM) and non-polarization maintaining single-mode fiber (SM) performance. For the latter case the Raman gain coefficient was halved, assuming totally unpolarized light propagating in the fiber [20]. While this approximation is probably too pessimistic, as the light is not fully depolarized after the SM fiber in practice, it serves as a good boundary case example of what are the limitations of PM and SM fibers.

3.1. Pulse dynamics and limitations for Mamyshev regenerator systems

As an illustrative example of the pulse dynamics in Fig. 6 shows the temporal and spectral domain evolution of a Gaussian pulse propagation with 50 ps duration and 350 W of peak power in 500 m of SM fiber.

This example highlights several key features similar to all simulated cases, that underline the major limiting factors for Mamyshev regenerator systems. Initial propagation from 0 m to 167 m is dominated by the SPM spectral broadening and dispersion acting simultaneously, resulting in broadening of the pulse in the time domain from 50 ps to 80 ps. Simultaneously SRS starts to grow from the noise floor at −60 dB at the Raman gain maximum at 1115 nm (visible in the logarithmic plot), but the energy in the Raman peak is still relatively low that it has little effect on the pulse temporal shape. With further propagation, temporal broadening due to dispersion slows down the spectral broadening as the peak power is decreasing. At approximately 278 m, additional spectral sidelobes can be noticed near the signal spectrum. The sidelobes are caused by optical wave breaking (OWB) [20]. These are particularly apparent in the logarithmic plot (Fig. 6(c)), but can also be seen in the latter stages on the linear spectra as well (Fig. 6(b)). OWB is also apparent in the time domain with the pulse edges steepening and oscillatory structures appearing at the edges (Fig. 6(a)).

Also around 278 meters the exponential amplification of SRS leads to spectral power at 1115 nm being significant enough (−30 dB relative to the signal) to start causing a significant modulation in the leading edge of the pulse profile. In our simulations we limit the Raman sideband growth to −15 dB level by stopping the simulation when this level is reached. This level was chosen to be well below −10 dB, where significant pump depletion affects Raman dynamics [23], and where the Raman effects to the pulse temporal shape were still considered moderate.

Interestingly enough, after 333 m, OWB temporarily halts further spectral broadening and can even result in a slight decrease of the 3 dB bandwidth of the pulse, as four-wave mixing

Optics EXPRESS

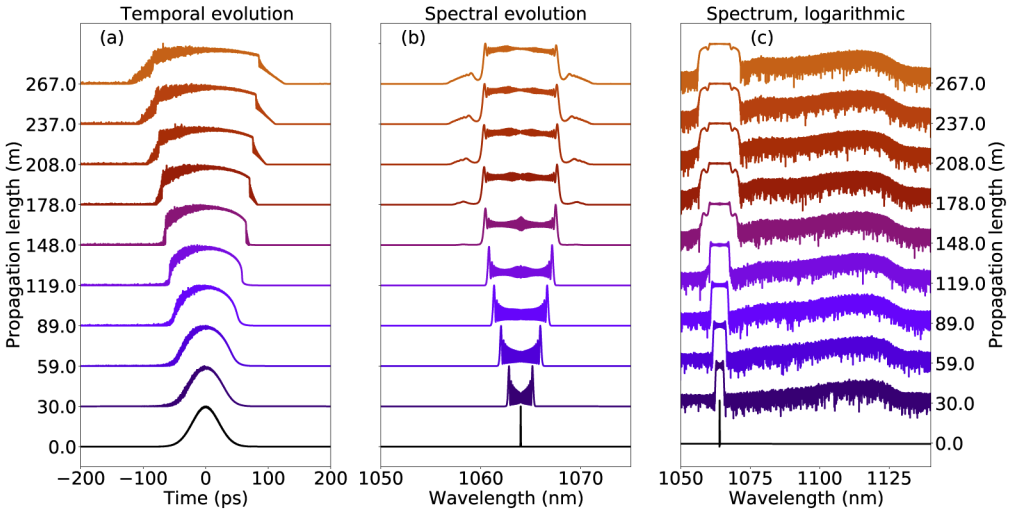

Fig. 6. Example of SPM broadening and SRS growth in SM fiber along the fiber length. Input pulse was 50 ps with 350 W peak power. (a) Pulse temporal intensity profile, (b) Linear spectrum, (c) Logarithmic spectrum. Intensities and spectra have been normalized for illustrative purposes.

from the edges of the spectra seed the OWB [20]. This can also be observed qualitatively in the linear spectra of Fig. 6 comparing the spectra after 333 m, showing no significant spectral broadening due to SPM. The 3 dB spectral bandwidth would stagnate or decrease until the OWB sidelobes' amplitude reach the −3 dB level, and consequently a sudden increase in the 3 dB bandwidth would be observed. However, this additional bandwidth is not useful anymore, as the nonlinear phase profile at the pulse edges could cause problems with further pulse shaping methods. Therefore we have imposed an additional limit condition for the propagation simulation in fiber, set by the length where OWB starts decreasing the bandwidth of the pulse.

Summarizing the above discussion, the simulations are performed with the pulse propagating in the fiber until one of the following three limit conditions is met:

1. **OWB condition:** The 3 dB bandwidth of the pulse starts to decrease due to OWB.
2. **Raman condition:** Highest peak in the SRS band at around 1115 nm rises above −15 dB level relative to the maximum.
3. **Maximum length condition:** Fiber length exceeds 500 m.

The last condition is set by practical constraints as fiber lengths in the excess of hundreds of meters are not very viable in real laser systems. Furthermore, longer fibers increase the pulse duration due to added dispersion, resulting in also longer pulse durations after filtering. This will consequently reduce the peak power of the filtered pulses making additional pulse shaping efforts difficult.

All simulations are launched with the given fiber and input pulse parameters and simulated until one of the three limiting conditions is triggered, which then stops the simulation at the given length. The stop conditions served to define the practical fiber length in Mamyshev regenerator resulting in varying output bandwidths, where the broadest spectrum is considered to be the optimum operating point.

Optics EXPRESS

4. Results and discussion

4.1. General behavior due to the limitations

We start our discussion by reviewing the results obtained in standard SM-980 and PM-980 fibers. Mode field diameter of the fiber is set at $MFD = 6.92\ \mu m$ and GVD at $\beta_2 = 0.024$ ps^2. As a simple approximation we use $A_{\text{eff}} \approx \pi(MFD/2)^2$ to evaluate the nonlinear coefficient. These values are close to commercially available fibers and serve as a good benchmark to understand the effect of different parameters on system behavior. The SM and PM cases were simulated by their different Raman gain coefficients, as mentioned earlier in the text. We first show the spectral broadening evolution for an initial pulse duration of 50 ps only with varying peak powers, as this helps to understand how the different limit cases are met arising from nonlinear effects along the propagation (Fig. 7). We have chosen 6 dB bandwidth as the metric as the 3 dB bandwidth is more prone to variations due to the rapid fluctuations of the SPM broadened spectrum combined with asymmetry caused by SRS.

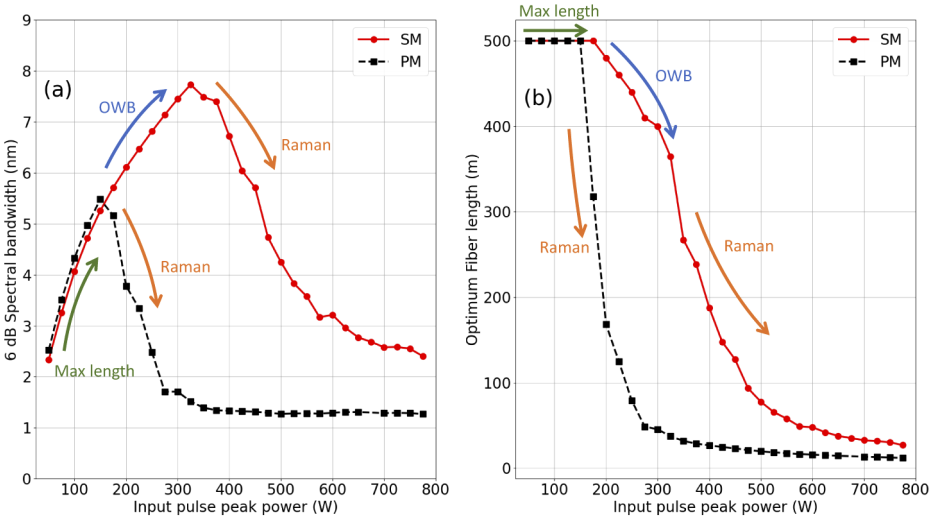

Fig. 7. (a) Example of evolution of bandwidth vs. input pulse peak power for 50 ps pulse in SM-980 fiber (red line, circles) and PM-980 (black line, squares). (b) Corresponding fiber length where simulation is terminated by the specified conditions.

Figure 7(a) shows the peak power of the pulse against the 6 dB bandwidth for both PM and SM fibers. Each point is defined by one of the stop conditions (OWB, Raman or Max. length). For peak powers ranging from 25 W to 150 W the 6 dB spectral bandwidth grows predictably with increasing power due to SPM (green arrow). When the peak power reaches 175 W we see a difference for the SM and PM fibers. For the SM fiber the bandwidth continues to grow (blue arrow), however the fiber length is limited due to OWB limit condition. For PM fibers we see already a decreasing 6 dB bandwidth beyond this point caused by the high power pulses reaching SRS threshold very rapidly. It is accompanied by a rapid decrease in the fiber length. The same effect occurs in SM fibers only at 325 W (red arrow).

Looking at Fig. 7(b), that illustrates the simulated fiber lengths corresponding to Fig. 7(a), we can verify the statements in the above paragraph. Up to 175 W both PM and SM fiber simulation lengths are limited by the 500 m limit condition. Beyond this point PM fiber lengths drop rapidly due to the Raman threshold condition, whereas SM fibers see a slower decline in fiber lengths due to the OWB condition. The Raman limit is achieved for the PM fiber faster due to the higher

Optics EXPRESS

Raman gain as discussed. Beyond 325 W we also observe a change in the slope of the SM fiber length, that corresponds to transition of the dominating limiting condition from OWB to Raman.

With increasing peak powers SRS grows even faster and the −15 dB threshold is reached before OWB has even cause significant effects on the pulse. This sets a stringent limit on the maximum fiber length, which can be used in the Mamyshev regenerator for pulse broadening, and consequently for the maximum obtainable bandwidth. As pointed out, the growth of the Raman sideband for higher peak powers is the reason why a careful balance of optimum peak power and fiber length is essential to achieve the broadest spectrum in Mamyshev regenerator systems.

4.2. Varying pulse duration in a standard fiber

Figure 8 demonstrates similar results as Fig. 7, but now for various pulse durations (20, 50, 80 and 100 ps). We observe several noteworthy features in the graphs. Firstly, the obtained maximum bandwidth for PM fiber is always lower than for SM fiber due to the difference in Raman gain. Secondly, shorter pulses will generally result in broader spectra compared to longer pulses for given input peak powers. This can be intuitively understood by larger spectral broadening due to the Kerr effect but also due to longer pulses suffering from longer walk-off length between the amplified SRS noise and the input pulse resulting in more net gain for SRS [20].

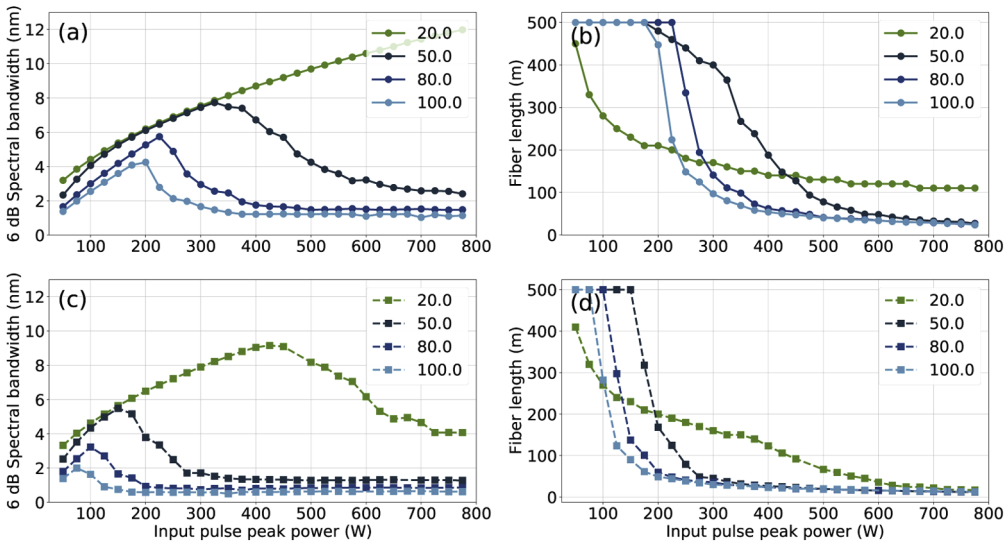

Fig. 8. Bandwidth and related maximum fiber length evolution for 20 ps, 50 ps, 80 ps and 100 ps pulses for different powers in SM-980 fiber (a,b) and PM-980 fiber (c,d).

Somewhat counterintuitively, this leads to the fact that when using longer pulses in a Mamyshev regenerator, increasing the peak power is a straightforward way to obtain broad spectra (considering the SRS and OWB limitations). The optimum operating point is obtained by optimizing the input pulse power in combination with fiber length. For example in Fig. 8(c) we note that for increasing pulse duration from 20 ps to 100 ps the optimum peak power (resulting in the broadest spectrum) decreases from 425 W to 75 W. The optimal fiber lengths are 110 m for 20 ps and 500 m for the rest. Even though the simulations for the longest pulses continue up to 500 m, the fiber can be made shorter in practice. The spectral broadening slows down during propagation in the fiber due to dispersion reducing the peak power, and nearly equivalent bandwidths could be obtained for the longer pulses with shorter fibers.

From a practical point of view, longer pulses will be significantly more difficult to use for regeneration, as the maximum obtainable broadening in can be only 2-5 nm. One should filter a

Optics EXPRESS

broad enough part from the side of the spectrum to be used as an efficient seed for further pulse shaping, while efficiently rejecting the incoherent part of the GSLD seed pulse at the center of the spectrum. Some ways to circumvent this problem is to either resort to SM fibers if the output polarization state is not crucial, to use additional pulse shaping stages at the cost of simplicity, or use different fibers that will affect the propagation dynamics. We will next look at the last option in more detail.

4.3. Effect of fiber parameters on optimum operating power

We start by setting the fiber dispersion to three values of $\beta_2 = 0.018ps^2$,$\beta_2 = 0.024ps^2$ (standard value of PM-980) and $\beta_2 = 0.03ps^2$ while maintaining the MFD of 6.9 μm. Typically adjusting the dispersion will also affect the fiber MFD, but for reasons of clarity we do not take this into account. In Fig. 9 we plot the 6 dB bandwidths for these three dispersion values.

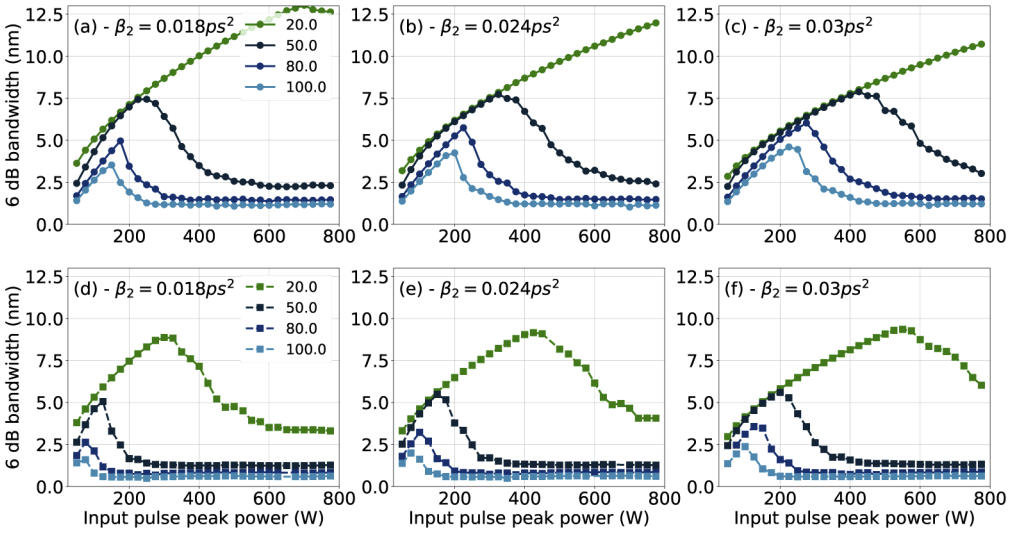

Fig. 9. Effect of dispersion on optimal bandwidth. Bandwidth evolution for 20 ps, 50 ps, 80 ps and 100 ps pulses for different input peak powers and different dispersion values in SM fiber (a,b,c) and PM fiber (d,e,f).

Comparing these results we note that the fiber dispersion has only minor effect on the maximum obtainable bandwidth for each pulse duration. However, the optimal input peak power is shifted towards higher powers with increasing dispersion. Increasing dispersion generally broadens the pulse in time domain faster, reducing the peak power. While this reduction in peak power is less favorable in terms of SPM, it also reduces the SRS growth rate. Hence, in order to achieve the same spectral bandwidth in fiber with higher dispersion, increased peak power is required. Simultaneously the reduced SRS allows one to use longer fiber lengths, effectively shifting the optimum position.

Following this, we now keep the dispersion constant at $\beta_2 = 0.024ps^2$ while varying the MFD to values of 5 μm and 10 μm. The results in this case, shown in Fig. 10, are similar when varying the dispersion. The maximum obtainable bandwidth is increasing only slightly with larger MFD. While this is again slightly counterintuitive, as one would expect smaller MFD (larger nonlinear coefficient) to cause larger spectral broadening, the reason can again be understood between the balance of SPM and SRS. Larger MFDs result in slower SRS growth rate, allowing one to use longer fibers for a given peak power resulting in larger spectral broadening, that could be achieved with a higher nonlinearity alone. Indeed, if we compare the spectral bandwidths at

Optics EXPRESS

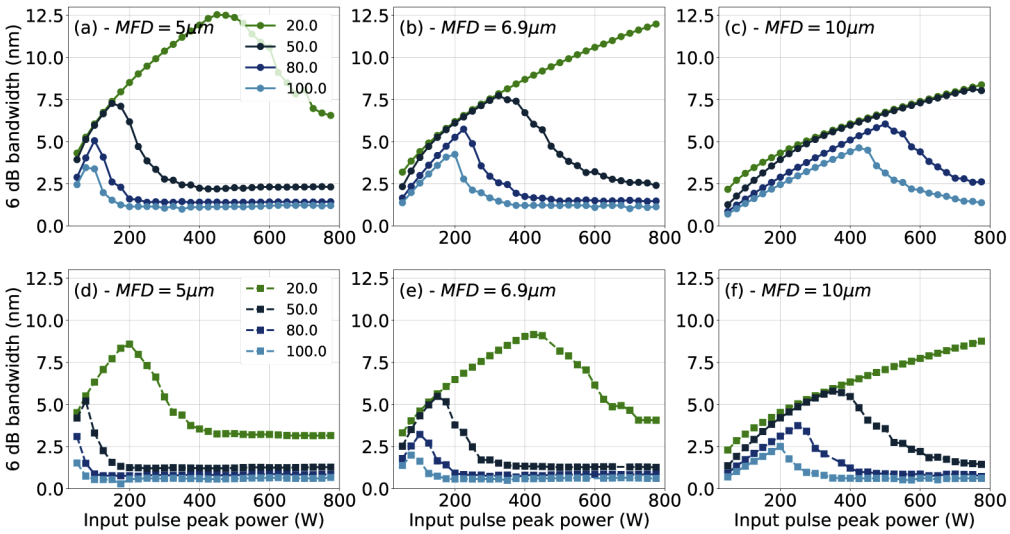

Fig. 10. Effect of the MFD of the fiber on optimum bandwidth. Bandwidth evolution for 20 ps, 50 ps, 80 ps and 100 ps pulses for different input peak powers and different MFD values in SM fiber (a,b,c) and PM fiber (d,e,f).

identical low peak power values, where SRS is not the limiting factor, smaller MFD will yield a broader spectrum.

5. Conclusions

We demonstrated experimentally pulse shortening down to <3 ps by a Mamyshev regenerator seeded by 80 ps GSD pulses. Such systems could provide an alternative way for pulse-on-demand applications requiring short pulse durations without mode-locked lasers. The system does not posses the pulse-to-pulse stability of mode-locked sources, but could be a viable option in applications where some fluctuations are allowed.

We have also studied the possibility of using different pulse durations and powers as well as various fiber configurations for Mamyshev regeneration schemes based on numerical simulations. The results indicate that for a given pulse duration an optimal input pulse peak power exists and should be used in order to achieve the largest spectral broadening, while keeping undesirable Raman noise levels down. Furthermore, the results show that reasonable spectral broadening (i.e. >5 nm) can be achieved with GSLD pulse durations below 50 ps. Longer pulses could also be used, but subsequent pulse filtering and nonlinear shaping steps need to be designed carefully to not enhance the already noisy seed source. Furthermore, improper filter design can result in double pulse structures due to the nature of the SPM broadened pulses. Optimizing the filter properties will be the subject of future studies.

While the choice of fiber has only minor effect on the maximum obtainable spectral broadening for a given pulse duration, the fiber parameters will affect the optimum peak power where this maximum is obtained. This optimum is a result of the delicate balance of SPM and dispersion affecting the pulse bandwidth and duration that, in turn, affect the total Raman gain seen by the amplified noise that depends on the dynamically changing walk-off length. Our results demonstrate the need for careful design of the pulse parameters for the system to work optimally.

Funding. Academy of Finland Flagship Programme, Photonics Research and Innovation (PREIN) (decision 320165);

Optics EXPRESS

European Commission Horizon 2020 Program PULSE project (824996); Ministry of Science and Higher Education of the Russian Federation (075-15-2020-934).

Acknowledgments. The authors wish to acknowledge CSC – IT Center for Science, Finland, for computational resources.

Disclosures. JF,TS and MG: PicoQuant (E).

References

1. M. Malinauskas, A. Žukauskas, S. Hasegawa, Y. Hayasaki, V. Mizeikis, R. Buividas, and S. Juodkazis, "Ultrafast laser processing of materials: from science to industry," Light: Science & Applications **5**(8), e16133 (2016).
2. K. Sugioka and Y. Cheng, "Ultrafast lasers—reliable tools for advanced materials processing," Light: Science & Applications **3**(4), e149 (2014).
3. Y. Jiang, S. Karpf, and B. Jalali, "Time-stretch lidar as a spectrally scanned time-of-flight ranging camera," Nat. Photonics **14**(1), 14–18 (2020).
4. Y.-S. Jang and S.-W. Kim, "Distance measurements using mode-locked lasers: A review," Nanomanuf. Metrol. **1**(3), 131–147 (2018).
5. X. Wei, B. Li, Y. Yu, C. Zhang, K. K. Tsia, and K. K. Y. Wong, "Unveiling multi-scale laser dynamics through time-stretch and time-lens spectroscopies," Opt. Express **25**(23), 29098–29120 (2017).
6. M. Närhi, B. Wetzel, C. Billet, S. Toenger, T. Sylvestre, J.-M. Merolla, R. Morandotti, F. Dias, G. Genty, and J. M. Dudley, "Real-time measurements of spontaneous breathers and rogue wave events in optical fibre modulation instability," Nat. Commun. **7**(1), 13675 (2016).
7. I. Coddington, N. Newbury, and W. Swann, "Dual-comb spectroscopy," Optica **3**(4), 414–426 (2016).
8. S. M. Link, D. J. H. C. Maas, D. Waldburger, and U. Keller, "Dual-comb spectroscopy of water vapor with a free-running semiconductor disk laser," Science **356**(6343), 1164–1168 (2017).
9. M. Becker, D. Kuizenga, and A. Siegman, "Harmonic mode locking of the nd:yag laser," IEEE J. Quantum Electron. **8**(8), 687–693 (1972).
10. G. Sobon, K. Krzempek, P. Kaczmarek, K. M. Abramski, and M. Nikodem, "10 GHz passive harmonic mode-locking in er–yb double-clad fiber laser," Opt. Commun. **284**(18), 4203–4206 (2011).
11. D. Korobko, D. Stoliarov, P. Itrin, M. Odnoblyudov, A. Petrov, and R. Gumenyuk, "Harmonic mode-locking fiber ring laser with a pulse repetition rate up to 12 GHz," Optics & Laser Technology **133**, 106526 (2021).
12. N. Uchida and N. Niizeki, "Acoustooptic deflection materials and techniques," Proc. IEEE **61**(8), 1073–1092 (1973).
13. W. J. Schwenger and J. M. Higbie, "High-speed acousto-optic shutter with no optical frequency shift," Rev. Sci. Instrum. **83**(8), 083110 (2012).
14. W. Fu, L. G. Wright, and F. W. Wise, "High-power femtosecond pulses without a modelocked laser," Optica **4**(7), 831–834 (2017).
15. P. V. Mamyshev, "All-optical data regeneration based on self-phase modulation effect," in *24th European Conference on Optical Communication. ECOC '98 (IEEE Cat. No.98TH8398)*, vol. 1 (1998), pp. 475–476 vol.1.
16. T. North and M. Rochette, "Regenerative self-pulsating sources of large bandwidths," Opt. Lett. **39**(1), 174–177 (2014).
17. K. Regelskis, J. Želudevičius, K. Viskontas, and G. Račiukaitis, "Ytterbium-doped fiber ultrashort pulse generator based on self-phase modulation and alternating spectral filtering," Opt. Lett. **40**(22), 5255–5258 (2015).
18. Z. Liu, Z. M. Ziegler, L. G. Wright, and F. W. Wise, "Megawatt peak power from a mamyshev oscillator," Optica **4**(6), 649–654 (2017).
19. P. Sidorenko, W. Fu, L. G. Wright, M. Olivier, and F. W. Wise, "Self-seeded, multi-megawatt, mamyshev oscillator," Opt. Lett. **43**(11), 2672–2675 (2018).
20. G. P. Agrawal, *Nonlinear Fiber Optics* (Academic Press, 2013).
21. J. M. Dudley, G. Genty, and S. Coen, "Supercontinuum generation in photonic crystal fiber," Rev. Mod. Phys. **78**(4), 1135–1184 (2006).
22. R. H. Stolen, J. P. Gordon, W. J. Tomlinson, and H. A. Haus, "Raman response function of silica-core fibers," J. Opt. Soc. Am. B **6**(6), 1159–1166 (1989).
23. Q. Li, H. Zhang, X. Shen, P. Yan, H. Hao, and M. Gong, "Stimulated raman scattering threshold for partially coherent light in silica fibers," Opt. Express **23**(22), 28438–28448 (2015).